SIGNAL ENHANCEMENT IN MEM RESONANT SENSORS USING PARAMETRIC SUPPRESSION

James M. L. Miller, Nicholas E. Bousse, Dongsuk D. Shin, Hyun-Keun Kwon, and Thomas W. Kenny
Department of Mechanical Engineering, Stanford University, Stanford, California, USA

ABSTRACT

We use parametric suppression for signal amplification in a phase-modulated microelectromechanical (MEM) charge detector. Simultaneously driving and parametrically pumping a MEM resonator with the appropriate relative phase increases the phase slope near the resonant frequency. We use this to increase the sensitivity of a MEM electrometer more than tenfold.

KEYWORDS

parametric amplification, electrometer, MEM resonator, perturbation theory, phase modulation

INTRODUCTION

Parametric enhancement is widely used for signal amplification of MEM resonant sensors, such as atomic force microscopes (AFMs) [1, 2, 3, 4], gyroscopes [5, 6, 7, 8], and magnetometers [9]. MEM resonators are often parametrically pumped by modulating the spring constant of a mode at twice its natural vibration frequency. Parametric pumping is phase-dependent, in contrast with mechanical pumping and the other phase-independent pumping strategies [10, 11, 12]. A parametric pump amplifies one quadrature of motion, while suppressing the other quadrature. This can be used to amplify signals in an amplitude-modulated (AM) configuration, provided that the signal frequency is close to the resonant frequency and the signal is in-phase with the pump [9]. The AM parametric enhancement strategy will amplify signals with minimal added noise and can improve the signal-to-noise ratio (SNR) of the measurement until the output signal is dominated by the thermomechanical noise, saturating at a thermomechanical SNR improvement of $\sqrt{2}$ at the onset of parametric oscillations [1, 9].

We demonstrate an alternate strategy for using parametric pumping to amplify signals in resonant sensors: phase-modulated (PM) parametric suppression. The resonator phase lag behind an external drive signal has a frequency-dependence that can be measured to infer shifts in the resonant frequency. This sensing strategy works by applying a drive signal of constant amplitude and frequency at resonance, and measuring the signal of interest via the phase shift that accompanies the corresponding resonant frequency shift [13]. Parametric enhancement increases the vibration amplitude but makes the phase slope less steep than the case without pumping, as is shown in Fig. 1. This contrasts with phase-independent feedback, where the increase in vibration amplitude is accompanied by an increase in phase slope [14, 15]. Parametric suppression makes the phase slope at resonance more steep than the case without pumping, as is shown in Fig. 2, so a PM resonant sensor will experience a larger shift in phase for the same shift in resonant frequency. While parametric suppression is clearly unsuitable for signal amplification in AM resonant sensors, it will amplify signals in sensing topologies that detect signals via a shift in the resonant frequency. We illustrate this amplification strategy by using parametric suppression to improve the signal of a PM resonant charge detector.

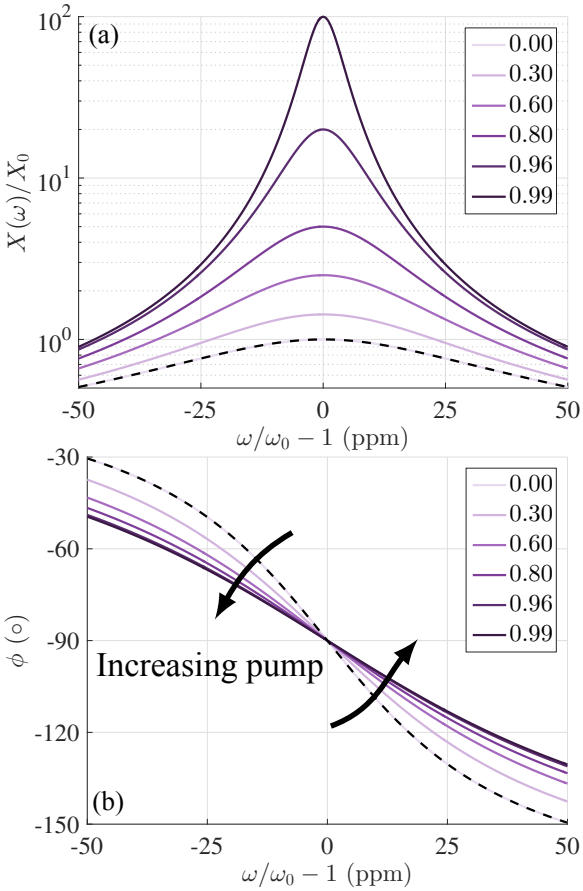

Figure 1: (a) Amplitude and (b) phase of a driven mechanical mode subjected to parametric enhancement, corresponding to $\psi = -\pi/4$ in Eq. 1. The legend specifies the normalized pump values, λ/λ_{thresh}, where λ_{thresh} is the parametric resonance threshold. The dashed line corresponds to the $\lambda = 0$ solution in Eqs. 2 and 3. The amplitude curves are normalized to the response in Eq. 2 at resonance, X_0.

MODEL

The dynamics of a single degree-of-freedom resonant system subjected to a direct drive and a parametric pump can be represented by:

$$\ddot{x} + \gamma\dot{x} + \omega_0^2 x + \lambda\cos(2\omega t)x = f\cos(\omega t + \psi), \quad (1)$$

where x is the displacement, $\omega_0 = \sqrt{k/m}$ is the natural frequency, $\gamma = \omega_0/Q$ is the damping rate, λ is the parametric pump strength, f is the direct drive force, ψ is the relative phase between the direct drive and the parametric pump, k is the spring constant, m is the effective mass, and Q is the inverse measure of dissipation known as the quality factor. The driven system without a pump ($\lambda = 0$) has a closed-form solution for the amplitude (X) and phase (ϕ) of the response:

$$X(\omega) = \frac{f}{\sqrt{(\omega_0^2 - \omega^2)^2 + \omega_0^2\gamma^2}}, \tag{2}$$

$$\phi(\omega) = \tan\left(\frac{\gamma\omega}{\omega^2 - \omega_0^2}\right). \tag{3}$$

To derive the response in the presence of a parametric pump, we first decompose the system response into two slowly-varying quadratures, $a(t)$ and $b(t)$:

$$x(t) = a(t)\cos(\omega t) + b(t)\sin(\omega t), \tag{4}$$

which must satisfy the following equation of constraint:

$$0 = \dot{a}(t)\cos(\omega t) + \dot{b}(t)\sin(\omega t). \tag{5}$$

We use the method of averaging to obtain the equations for $a(t)$ and $b(t)$, accurate to first order [16, 17]:

$$\dot{a} = -\frac{\omega b}{2} - \frac{\gamma a}{2} + \frac{\omega_0^2 b}{2\omega} - \frac{\lambda b}{4\omega} + \frac{f\sin(\psi)}{2\omega}, \tag{6}$$

$$\dot{b} = \frac{\omega a}{2} - \frac{\gamma b}{2} - \frac{\omega_0^2 a}{2\omega} - \frac{\lambda a}{4\omega} + \frac{f\cos(\psi)}{2\omega}, \tag{7}$$

The steady-state response can be obtained by setting $\dot{a} = 0$ and $\dot{b} = 0$ in Eqs. 6 and 7, and numerically solving for $a(\omega)$ and $b(\omega)$ for a given resonant frequency, damping rate, pump strength, drive strength, and phase between the pump and drive. The two quadratures can finally be converted to an amplitude and phase using $X = a^2 + b^2$ and $\tan(\phi) = b/a$.

Figures 1 and 2 plot the solutions to Eqs. 6 and 7 for increasing values of λ and a relative phase that yields maximum parametric enhancement ($\psi = -\pi/4$) and maximum parametric suppression ($\psi = \pi/4$), respectively. Beyond the onset of parametric resonance, λ_{thresh}, the quadrature of motion in-phase with the pump parametrically resonates, and additional nonlinearities must be incorporated into Eq. 1 to bound the response [18, 19]. Fig. 2(b) shows that for parametric suppression, the change in phase for a small change in frequency near the resonant frequency can be amplified with increasing pump strength.

EXPERIMENT AND DISCUSSION

We use parametric suppression for signal amplification in the MEM torsional electrometer depicted in Fig. 3. Micromechanical electrometers have reached single electron sensitivities, exceeding the sensitivities of commercial charge detectors by several orders of magnitude [20, 21, 22]. Our electrometer is fabricated

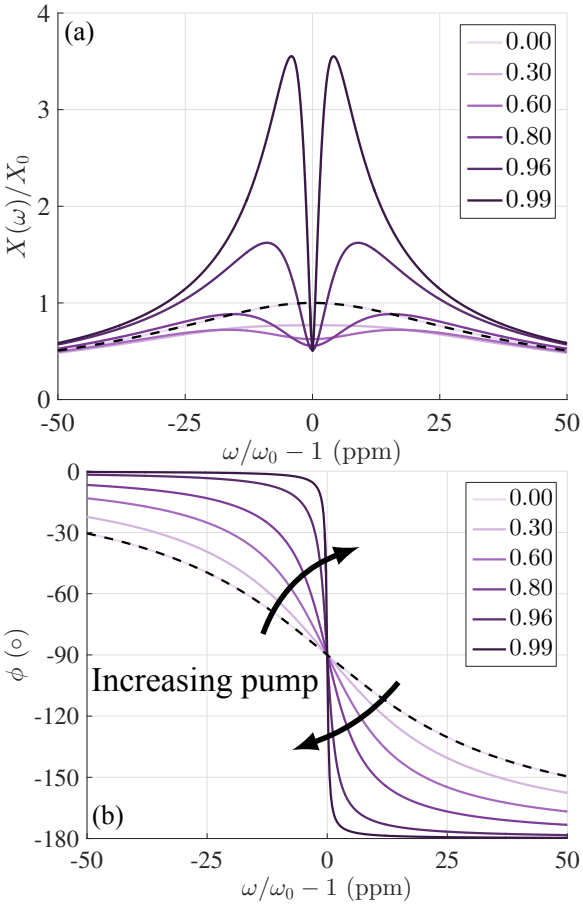

Figure 2: (a) Amplitude and (b) phase of a driven mechanical mode subjected to parametric suppression.

within a wafer-scale encapsulation process that produces high-Q devices in a hermetic vacuum-sealed environment [23]. The device is anchored at two points, and resonates via a torsional mode that modifies the capacitance to the sense electrodes. When a bias voltage is applied between the vibrating element and the sense electrodes, this induces a motional current that can be amplified to measure the displacement. A series of internal electrodes are etched out of the vibrating element to increase the sensitivity of the capacitive readout. We use two sets of these internal electrodes to differentially transduce the motional current. This enables us to easily resolve the thermomechanical displacement noise in Fig. 4 using a bias voltage of only 4 V, comparable to the available voltages in handheld consumer electronic devices.

A mechanical resonator can be used to measure an external signal, such as a nearby distribution of charges, via a change in the resonant frequency of one of its mechanical modes. In our device, as the voltage difference between the top left electrode and suspended element increases, the resonant frequency decreases via electrostatic softening. This is demonstrated in Fig. 4, showing that the peak thermomechanical noise frequency decreases with increasing voltage difference.

The device responses in Fig. 5 confirm the model plotted in Figs. 1 and 2. We use the top right electrode to sweep an external constant drive across resonance while simultaneously applying a parametric pump of

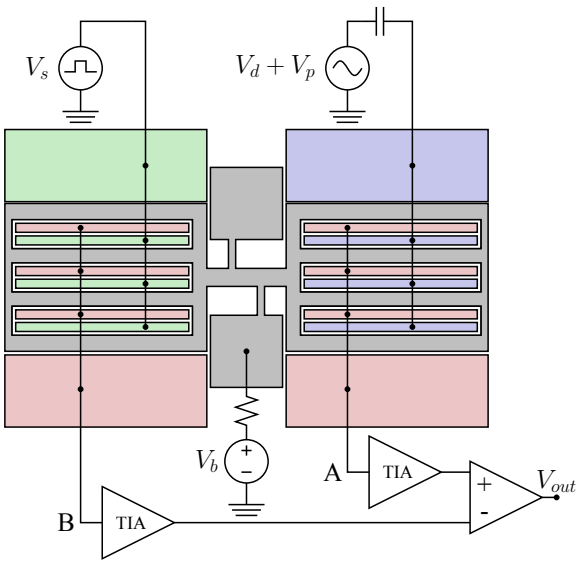

Figure 3: The schematic of the fabricated resonator. The biased device is forced and pumped with the top right electrode, and differentially sensed via two transimpedance amplifiers (TIAs) using the bottom left and right electrodes. A square wave voltage is applied to the top left electrode to slowly vary the spring constant.

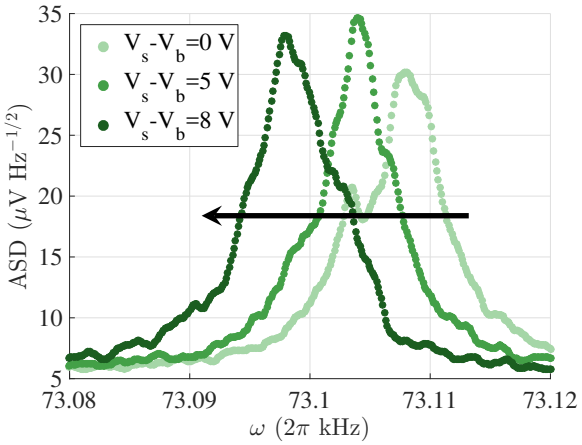

Figure 4: The thermomechanical noise amplitude spectral density (ASD) with varying electrode bias.

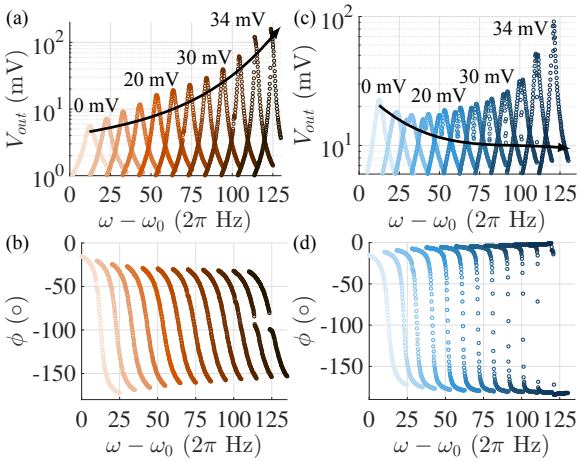

Figure 5: (a, c) The amplitude-frequency curves for parametric enhancement and suppression, respectively, showing an increase (decrease) in the amplitude at resonance with increasing pump strength. (b, d) The phase-frequency curves, showing a decrease (increase) in phase-slope with increasing pump. The curves are each shifted forward by 10 Hz to better illustrate the dynamics with pumping.

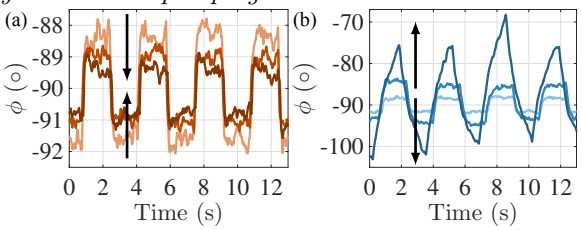

Figure 6: Charge detection using a drive (at ω_0) and pump (at $2\omega_0$) applied to the top right electrode and a 50 mV amplitude, 300 mHz frequency square wave voltage applied to the top left electrode. The pump amplitudes (in order of increasing shading) are 0 mV, 20 mV, and 30 mV. Parametric oscillations occur at approximately 31 mV. Increasing parametric (a) enhancement, and (b) suppression reduces (increases) the phase amplitude for a given square wave amplitude.

increasing amplitude at twice the drive frequency. In Fig. 5(a-b), the pump is in-phase with the driven quadrature of motion, so increasing the pump strength increases the amplitude but reduces the phase slope. In Fig. 5(c-d), the pump is orthogonal to the drive quadrature, which suppresses the amplitude at resonance while increasing the phase slope.

We employ parametric suppression to increase device charge sensitivity via the slope detection technique [13]. We measure $\omega_0(t_0)$ of the torsional mode by grounding the top left electrode, and then apply to the top right electrode a drive and pump at $\omega_0(t_0)$ and $2\omega_0(t_0)$, respectively. Changes in the top left electrode voltage will now shift the resonant frequency to a new value, $\omega_0(t)$, which in turn shifts the phase lag of the displacement behind the drive. In Fig. 6, we apply a square wave voltage to the top left electrode to modulate $\omega_0(t)$ at well below the resonant frequency; this is the signal of interest. In Fig. 6(a), increasing the parametric enhancement causes the phase signal to decrease, even though the amplitude at resonance increases. In Fig. 6(b), increasing the parametric suppression causes the phase signal to increase, even though the amplitude at resonance decreases. At pump amplitudes near threshold, the sensitivity is increased tenfold while the sensor bandwidth decreases below the charge modulation rate.

Parametric suppression can be leveraged to amplify the response of PM sensors that detect signals via a shift in the resonant frequency, such as AFMs, electrometers, and mass sensors. However, parametric suppression will simultaneously amplify the intrinsic frequency noise [24]. The SNR will saturate once the error in the phase detection is negligible compared to the amplified intrinsic frequency noise.

Acknowledgments

Fabrication was performed in the nano@Stanford labs, which are supported by the National Science Foundation (NSF) as part of the National Nanotechnology Coordinated Infrastructure under award ECCS-

1542152, with support from the Defense Advanced Research Projects Agency Precise Robust Inertial Guidance for Munitions (PRIGM) Program, managed by Ron Polcawich and Robert Lutwak. J.M.L.M. is supported by the National Defense Science and Engineering Graduate (NDSEG) Fellowship and the E.K. Potter Stanford Graduate Fellowship. J.M.L.M. is grateful to Guillermo Villanueva, Steven Shaw, and Daniel Rugar for helpful discussions.

REFERENCES

[1] D. Rugar and P. Grütter, "Mechanical parametric amplification and thermomechanical noise squeezing," *Phys. Rev. Lett.*, vol. 67, pp. 699–702, 1991.

[2] K. L. Turner, S. A. Miller, P. G. Hartwell, N. C. MacDonald, S. H. Strogatz, and S. G. Adams, "Five parametric resonances in a microelectromechanical system," *Nature*, vol. 396, p. 149, 1998.

[3] G. Prakash, A. Raman, J. Rhoads, and R. G. Reifenberger, "Parametric noise squeezing and parametric resonance of microcantilevers in air and liquid environments," *Rev. Sci. Instrum.*, vol. 83, p. 065109, 2012.

[4] D. I. Caruntu, I. Martinez, and M. W. Knecht, "Parametric resonance voltage response of electrostatically actuated micro-electro-mechanical systems cantilever resonators," *J. Sound Vib.*, vol. 362, pp. 203–213, 2016.

[5] Z. X. Hu, B. J. Gallacher, J. S. Burdess, C. P. Fell, and K. Townsend, "A parametrically amplified MEMS rate gyroscope," *Sens. Actuators A*, vol. 167, no. 2, pp. 249–260, 2011.

[6] S. H. Nitzan, V. Zega, M. Li, C. H. Ahn, A. Corigliano, T. W. Kenny, and D. A. Horsley, "Self-induced parametric amplification arising from nonlinear elastic coupling in a micromechanical resonating disk gyroscope," *Sci. Rep.*, vol. 5, p. 9036, 2015.

[7] D. Senkal, E. J. Ng, V. Hong, Y. Yang, C. H. Ahn, T. W. Kenny, and A. M. Shkel, "Parametric drive of a toroidal mems rate integrating gyroscope demonstrating $<$ 20 ppm scale factor stability," in *28th IEEE Int. Conf. Microelectromech. Syst.*, pp. 29–32, 2015.

[8] M. Song, B. Zhou, Z. Chen, H. Wang, T. Zhang, and R. Zhang, "Parametric drive MEMS resonator with closed-loop vibration control at ambient pressure," in *IEEE Int. Symp. Inertial Sens. Syst.*, pp. 85–88, 2016.

[9] M. J. Thompson and D. A. Horsley, "Parametrically amplified z-axis Lorentz force magnetometer," *J. Microelectromech. Syst.*, vol. 20, pp. 702–710, 2011.

[10] A. Olkhovets, D. Carr, J. Parpia, and H. Craighead, "Non-degenerate nanomechanical parametric amplifier," in *14th IEEE Int. Conf. Microelectromech. Syst.*, pp. 298–300, 2001.

[11] M. Napoli, W. Zhang, K. Turner, and B. Bamieh, "Dynamics of mechanically and electrostatically coupled microcantilevers," in *12th IEEE Int. Conf. Solid-State Sens. Actuators Microsyst. (Transducers)*, vol. 2, pp. 1088–1091, 2003.

[12] J. M. L. Miller, A. Ansari, D. B. Heinz, Y. Chen, I. B. Flader, D. D. Shin, L. G. Villanueva, and T. W. Kenny, "Effective quality factor tuning mechanisms in micromechanical resonators," *Appl. Phys. Rev.*, vol. 5, p. 041307, 2018.

[13] T. R. Albrecht, P. Grütter, D. Horne, and D. Rugar, "Frequency modulation detection using high-Q cantilevers for enhanced force microscope sensitivity," *J. Appl. Phys.*, vol. 69, no. 2, pp. 668–673, 1991.

[14] J. Tamayo, A. D. L. Humphris, R. J. Owen, and M. J. Miles, "High-Q dynamic force microscopy in liquid and its application to living cells," *Biophys. J.*, vol. 81, no. 1, pp. 526–537, 2001.

[15] J. M. L. Miller, H. Zhu, D. B. Heinz, Y. Chen, I. B. Flader, D. D. Shin, J. E.-Y. Lee, and T. W. Kenny, "Thermal-piezoresistive tuning of the effective quality factor of a micromechanical resonator," *Phys. Rev. Applied*, vol. 10, p. 044055, 2018.

[16] A. H. Nayfeh and D. T. Mook, *Nonlinear oscillations*. John Wiley & Sons, 2008.

[17] M. V. Requa and K. L. Turner, "Electromechanically driven and sensed parametric resonance in silicon microcantilevers," *Appl. Phys. Lett.*, vol. 88, p. 263508, 2006.

[18] J. F. Rhoads and S. W. Shaw, "The impact of nonlinearity on degenerate parametric amplifiers," *Appl. Phys. Lett.*, vol. 96, p. 234101, 2010.

[19] Z. R. Lin, Y. Nakamura, and M. I. Dykman, "Critical fluctuations and the rates of interstate switching near the excitation threshold of a quantum parametric oscillator," *Phys. Rev. E*, vol. 92, p. 022105, 2015.

[20] A. N. Cleland and M. L. Roukes, "A nanometre-scale mechanical electrometer," *Nature*, vol. 392, no. 6672, p. 160, 1998.

[21] P. S. Riehl, K. L. Scott, R. S. Muller, R. T. Howe, and J. A. Yasaitis, "Electrostatic charge and field sensors based on micromechanical resonators," *J. Microelectromech. Syst.*, vol. 12, no. 5, pp. 577–589, 2003.

[22] J. Lee, Y. Zhu, and A. Seshia, "Room temperature electrometry with sub-10 electron charge resolution," *J. Micromech. Microeng.*, vol. 18, no. 2, p. 025033, 2008.

[23] Y. Yang, E. J. Ng, Y. Chen, I. B. Flader, and T. W. Kenny, "A unified epi-seal process for fabrication of high-stability microelectromechanical devices," *J. Microelectromech. Syst.*, vol. 25, pp. 489–497, 2016.

[24] A. N. Cleland and M. L. Roukes, "Noise processes in nanomechanical resonators," *J. Appl. Phys.*, vol. 92, no. 5, pp. 2758–2769, 2002.

Email: jmlm@stanford.edu